International Tables for Crystallography (2006). Vol. C, Figure 2.7.2.4, p. 117.

diffraction in $CC'D'D$ will take the path shown by the heavy line in Fig. 2.7.2.4, simplifying the picture to the case of extreme confinement of energy flow to parallelism with the Bragg planes. At the X-ray exit surface DD', splitting into $\mathbf{K}_0$ and $\mathbf{K}_h$ beams occurs. A slit-less arrangement, as shown in the figure, may suffice. Then, when S is a point-like source of $K\alpha$ radiation, and distance a is sufficiently large, films F_1 and F_2 will each record a pair of narrow images formed by the α_1 and α_2 wavelengths, respectively. A wider area of specimen can be imaged if a line focus rather than a point focus is placed at S (Barth & Hosemann, 1958), but then the α_1 and α_2 images will overlap. Under conditions of high anomalous transmission, defects in the crystal cause a reduction in transmitted intensity, which appears similarly in the $\mathbf{K}_0$ and $\mathbf{K}_h$ images. Thus, it is possible to gain intensity and improve resolution by recording both images superimposed on a film F_3 placed in close proximity to the X-ray exit face DD' (Gerold & Meier, 1959).

2.7.3. Double-crystal topography

The foregoing description of single-crystal techniques will have indicated that in order to gain greater sensitivity in orientation contrast there are required incident beams with closer collimation, and limitation of dispersion due to wavelength spread of the characteristic X-ray lines used. It suggests turning to prior reflection of the incident beam by a perfect crystal as a means of meeting these needs. Moreover, the application of crystal-reflection-collimated radiation to probe angularly step by step as well as spatially point by point the intensity of Bragg reflection from the vicinity of an individual lattice defect such as a dislocation brings possibilities of new measurements beyond the scope provided by simply recording the local value of the integrated reflection. The X-ray optical principles of double-crystal X-ray topography are basically those of the double-crystal spectrometer (Compton & Allison, 1935). The properties of successive Bragg reflection by two or more crystals can be effectively displayed by a Du Mond diagram (Du Mond 1937), and such will now be applied to show how collimation and monochromatization result from successive reflection by two crystals, U and V, arranged as sketched in Fig. 2.7.3.1. They are in the dispersive, antiparallel, '$++$' setting, and are assumed to be identical perfect crystals set for the same symmetrical Bragg reflection. Only rays making the same glancing angle with both surfaces will be reflected by both U and V. For example, radiation of shorter wavelength reflected at a smaller glancing angle at U (the ray shown by the dashed line) will impinge at a larger glancing angle on V and not satisfy the Bragg condition. In this $++$ setting, with a given angle ω between the Bragg-reflecting planes of each crystal, $\theta_U + \theta_V = \omega$ and $\Delta\theta_U = -\Delta\theta_V$. The Du Mond diagram for the $++$ setting, Fig. 2.7.3.2, shows plots of Bragg's law for each crystal, the V curve being a reflection of the U curve in a vertical mirror line and differing by ω from the U curve in its coordinate of intersection with the axis of abscissa, in accord with the equations given above. The small angular range of reflection of a monochromatic ray by each perfect crystal is represented exaggeratedly by the band between the parallel curves. Where the band for crystal U superimposes on the band for V (the shaded area) defines semiquantitatively the divergence and wavelength spread in the rays successively reflected by U and V. (It is taken for granted that $\frac{1}{2}\omega$ lies between the maximum and minimum incident glancing angles on U, $\theta_{\max}$ and $\theta_{\min}$, afforded by the incident beam, assumed polychromatic.) The reflected beam from U alone contains wavelengths ranging from $\lambda_{\min}$ to $\lambda_{\max}$. Comparison of these θ and λ ranges with the extent of the shaded area illustrates the efficacy of the $++$ arrangement in providing a collimated and monochromatic beam, which can be employed to probe the reflecting properties of a third crystal (Nakayama, Hashizume, Miyoshi, Kikuta & Kohra, 1973). Techniques employing three or more successive Bragg reflections find considerable application when used with synchrotron X-ray sources, and will be considered below, in Section 2.7.4.

The most commonly used arrangement for double-crystal topography is shown in Fig. 2.7.3.3, in which U is the 'reference' crystal, assumed perfect, and V is the specimen crystal under examination. Crystals U and V are in the parallel, '$+-$' setting, which is non-dispersive when the Bragg planes of U and V have the same (or closely similar) spacings. Before considering the Du Mond diagram for this arrangement, note that Bragg reflection at the reference crystal U is asymmetric, from planes inclined at angle α to its surface. Asymmetric reflections have useful properties, discussed, for example, by Renninger (1961), Kohra (1972), Kuriyama & Boettinger (1976), and Boettinger, Burdette & Kuriyama (1979). The asymmetry factor, b, of magnitude $|\mathbf{K}_0 \cdot \mathbf{n}/\mathbf{K}_h \cdot \mathbf{n}|$, $\mathbf{n}$ being the

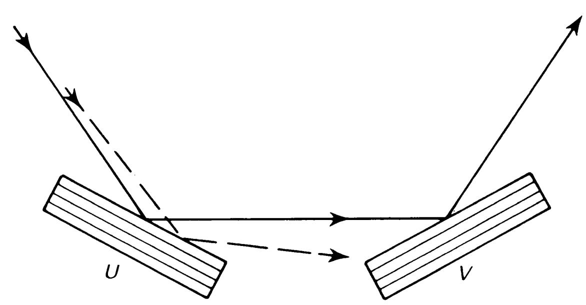

Fig. 2.7.3.1. Double-crystal $++$ setting.

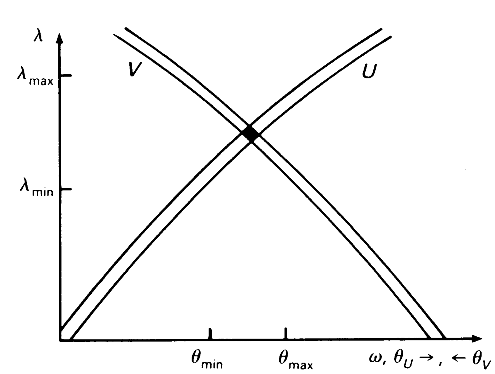

Fig. 2.7.3.2. Du Mond diagram for $++$ setting in Fig. 2.7.3.1.

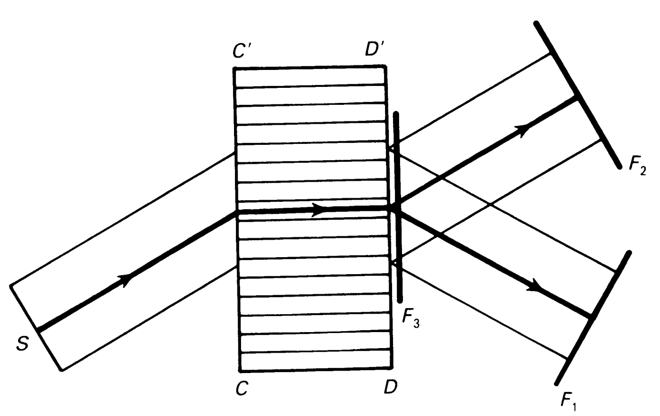

Fig. 2.7.2.4. Topographic techniques using anomalous transmission.

references